ORIGINAL SCIENTIFIC PAPER

CROATICA CHEMICA ACTA

Croat. Chem. Acta **2026**, *99*(4)
Published online: November 20, 2026
DOI: 10.5562/cca4278

HKD 1926

Antiproliferative Evaluation of Mono- and Disubstituted Ferrocene Derivatives with Aldoxime Ether- and Ester-Linked Five-Membered Heterocycles

Martina Piškor Benković,[1] Silvija Maračić,[1] Mario Cetina,[2] Dijana Jadreško,[3] Sandra Kraljević Pavelić,[4] Krešimir Pavelić,[5] Silvana Raić-Malić[1,*]

[1] University of Zagreb Faculty of Chemical Engineering and Technology, Department of Organic Chemistry, Marulićev trg 20, 10000, Zagreb, Croatia
[2] University of Zagreb Faculty of Textile Technology, Department of Applied Chemistry, Prilaz Baruna Filipovića 28a, 10000, Zagreb, Croatia
[3] Ruđer Bošković Institute, Division for Marine and Environmental Research, Bijenička cesta 54, 10000, Zagreb, Croatia
[4] University of Rijeka Faculty of Health Studies, Viktora Cara Emina 5, 51000, Rijeka, Croatia
[5] Juraj Dobrila University of Pula Faculty of Medicine, Zagrebačka 30, 52100, Pula, Croatia
* Corresponding author's e-mail address: sraic@fkit.unizg.hr

RECEIVED: February 2, 2026 * REVISED: September 8, 2026 * ACCEPTED: September 13, 2026

THIS PAPER IS DEDICATED TO THE MEMORY OF OLGA KRONJA (1953 – 2025)

Abstract: Mono- and disubstituted ferrocene derivatives linked to five-membered heterocycles via aldoxime ether or ester linkers were synthesized by a Cu(I)-catalyzed 1,3-dipolar cycloaddition using a mechanochemical liquid-assisted grinding (LAG) approach. The structures of the compounds were confirmed by NMR spectroscopy, mass spectrometry, and single-crystal X-ray diffraction. Antiproliferative activity *in vitro* was evaluated against the non-small lung cancer (H460), metastatic colorectal adenocarcinoma (SW620), hepatocellular carcinoma (HepG2) and breast cancer (MCF-7) cell lines, as well as non-tumor human embryonic kidney (HEK293T) cells. Disubstituted ferrocene derivatives exhibited higher antiproliferative activity than their monosubstituted analogs, particularly against HepG2 and MCF-7 cells, with several compounds demonstrating activity in the low micromolar range. The highest selectivity toward HepG2 cells was observed for ester derivative **9f**, bearing an *N*-methylpyrrolyl substituent (IC_{50} = 5 μM, selectivity index, SI > 20). Electrochemical analysis confirmed the quasi-reversible oxidation of ferrocene unit, followed by irreversible processes associated with the triazole core, suggesting that the redox-active ferrocene core is a plausible but as yet unconfirmed contributor to biological activity.

Keywords: ferrocene, five-membered heterocycles, triazole, CuAAC, mechanochemistry, antiproliferative activity.

INTRODUCTION

FERROCENE, a well-established organometallic compound with a central iron atom between two cyclopentadienyl rings, has proven to be a highly versatile scaffold for drug development. Its excellent thermal and oxidative stability, reversible redox properties, and high lipophilicity make it particularly valuable for medicinal applications.[1,2] These features contribute to favorable pharmacokinetics, including enhanced membrane permeability and the ability to cross the blood–brain barrier.[3,4] One of the most successful strategies in drug design has been the substitution of planar aromatic groups with ferrocenyl moieties.[5–8] In contrast to planar aromatic rings, the barrel-shaped structure of a metallocene allows for more effective filling of hydrophobic cavities, in a manner that phenyl or other (hetero)aromatic moieties cannot, often enhancing molecular interactions and improving biological activity.[9] This bioisosteric replacement approach has led to the development of several ferrocene-containing antimalarial and anticancer agents.[10–12] For instance, replacing the phenyl ring in chloroquine with a ferrocene unit resulted in ferroquine, which shows improved activity against chloroquine-resistant *Plasmodium* strains. Similarly, introducing a ferrocenyl group into selective estrogen receptor

This work is licensed under a Creative Commons Attribution 4.0 International License.

modulators (SERMs) yielded derivatives with potent cytotoxic effects against both hormone-dependent and hormone-independent breast cancers.[13–17] Integration of ferrocene into therapeutic scaffolds has progressively expanded across various pharmacophores, contributing to the identification of compounds with pronounced antiproliferative activity against a broad range of cancer cell lines.[12,18–23] Mechanistically, ferrocene-based anticancer agents act through multiple pathways. These include redox cycling to generate reactive oxygen species (ROS), induction of oxidative stress, mitochondrial disruption, and inhibition of redox-regulating enzymes like thioredoxin reductase. Additional effects involve the activation of apoptosis via cytochrome c release, modulation of signaling pathways such as PI3K/Akt and JNK, and cell cycle arrest in the G_2/M phase.[12,24–27]

Among heterocycles commonly used in drug design, pyrroles are frequently found in kinase inhibitors and DNA-interacting agents due to their high electron density and strong target-binding potential.[28,29] Thiophene serves as a sulfur-containing phenyl bioisostere that improves metabolic stability and drug target interactions. Furan contributes unique π-electron properties and oxidative sensitivity, supporting redox-mediated mechanisms of cytotoxicity.[30–32] In addition, the use of 1,2,3-triazole as a chemically stable linker has become a popular strategy for the synthesis of hybrid molecules. Formed by Cu(I)-catalyzed azide–alkyne cycloaddition (CuAAC), triazole is resistant to oxidative, reductive and, hydrolytic degradation and is well suited for drug discovery due to its ability to form multiple non-covalent interactions, including hydrogen bonding and π-stacking.[33] Triazole-containing compounds exhibit a broad spectrum of pharmacological activities, including anticancer activity via inhibition of tyrosine kinases, BET proteins and microtubule dynamics. In addition, oxime ether and ester linkers offer distinct pharmacological advantages in heterocyclic hybrids.[33,34] Oxime ethers are known for their structural versatility and have shown cytotoxic activity against various cancer cell lines such as breast, prostate, leukemia and lung. These derivatives act through both hormonal and non-hormonal pathways and are included in several FDA-approved drugs.[35–37] Ester linkers, on the other hand, are often used in drug conjugates due to their enzyme-cleavable nature and allow selective activation in cancer cells rich in lysosomal esterase.[38,39]

The antiproliferative activity observed in our previous studies[40–45] on ferrocene–heterocycle hybrids linked via a 1,2,3-triazole moiety prompted the synthesis of structurally related analogues with the aim of obtaining improved cytostatic activity (Figure 1).

Building on these findings, we designed and investigated mono- and disubstituted ferrocene derivatives bearing five-membered heterocycles with ester or aldoxime ether linkers, emphasizing mechanochemical synthesis, structural characterization, electrochemical analysis and *in vitro* antiproliferative evaluation.

MATERIALS AND METHODS

General

Mechanochemical reactions were carried out using an IST400 (InSolido Tehnologies, Croatia) mixer mill operating at 30 Hz in stainless steel reaction vessels using stainless steel balls. All the starting chemicals, reagents and solvents were purchased from commercial suppliers. For monitoring the progress of a reaction, analytical thin layer chromatography (TLC) was performed on Merck pre-coated silica gel 60-F254 aluminum plates. Visualization of the spots on TLC plates was achieved by exposure to UV light (254 nm). Column chromatography was done using Fluka (Buchs, Switzerland) silica gel (0.063–0.2 mm) and Merck (Darmstadt, Germany) aluminum oxide (Al_2O_3, 0.063–0.2 mm), glass columns were slurry-packed under gravity. ^{1}H and ^{13}C NMR spectra were acquired on a Bruker Biospin (Rheinstetten, Germany) NMR spectrometer. All data were recorded in DMSO-d_6 at 298 K. The chemical shifts are relative to residual solvent signal DMSO-d_6 at δ = 2.50 ppm for ^{1}H and δ = 39.50 ppm for ^{13}C. Individual resonances were assigned based on their chemical shifts, signal intensities, multiplicities of resonances and H–H coupling constants. ^{1}H- and ^{13}C-NMR spectra of compounds, **2a–c**, **3b**, **3c**, **3e**, **3f**, **5a–c**, **6a–f**, **8a–c** and **9a–f**, are provided in Figures S1–S25. The high-resolution mass spectra (HRMS) of the final compounds were recorded using an Applied Biosystems ESI Q-TOF analyzer, and are provided in Figures S26–S43.

Aldoxime derivatives (**1a–c**) were synthesized according to known procedures,[46,47] and the obtained mixture of isomers was separated by column chromatography. Azido precursors, 1-azidomethyl-ferrocene (**4**) and 1,1'-bis(azidomethyl)ferrocene (**7**), were also synthesized according to well-known procedures.[44,48]

Experimental Procedures for the Synthesis of Compounds

Synthesis of *O*-propargylated heterocyclic derivatives 2a–c and 3a–f

O-propargylated furan-2-carboxylic acid and thiophene-2-carboxylic acid (**3a**, **3d**) are known compounds[49,50] synthesized according to the modified reaction conditions shown in the general procedure for the *O*-propargylation.

General procedure for the *O*-propargylation of heterocyclic aldoxime and carboxylic acids (2a–c, 3b, 3c, 3e, 3f)

To a solution of the corresponding heterocyclic aldoxime or carboxylic acid (1 equiv.) in dry dimethylformamide (DMF), potassium carbonate (K_2CO_3, 1.2 equiv.) was added, and the reaction mixture was stirred at room temperature for 1 h. Propargyl bromide (1.2 equiv.) was then added, and stirring was continued overnight. Upon completion, the reaction mixture was quenched and extracted with ethyl acetate (EtOAc). The combined organic layers were washed with water (×2), dried over anhydrous sodium sulfate (Na_2SO_4), and concentrated under reduced pressure. The resulting crude ester derivatives were used without further purification, whereas the aldoxime ethers were purified by column chromatography.

2-Thiophenecarboxaldehyde *O*-2-propyn-1-yloxime (2a). Compound **2a** was synthesized according to the general procedure using (*E*)-thiophene-2-carbaldehyde oxime **1a** (133 mg, 1.05 mmol), propargyl bromide (149 mg, 1.26 mmol) and K_2CO_3 (173 mg, 1.26 mmol). After column chromatography (CH_2Cl_2 : MeOH = 100 : 1), compound **2a** was isolated as a yellow powder (69 mg, 40 %, m.p. = 96–98 °C).^{1}H-NMR (600 MHz, DMSO) *δ*/ppm*:* 8.00 (s, 1H, –C<u>H</u>=N–), 7.85 (dt, *J* = 5.1, 1.1 Hz, 1H, H-5), 7.57 (dd, *J* = 3.7, 1.0 Hz, 1H, H-3), 7.18 (dd, *J* = 5.1, 3.7 Hz, 1H, H-4), 4.84 (d, *J* = 2.4 Hz, 2H, C<u>H</u>$_2$), 3.52 (t, *J* = 2.4 Hz, 1H, C<u>H</u>). ^{13}C-NMR (151 MHz, DMSO) *δ*/ppm*:* 140.75, 132.71, 132.15, 129.81, 126.09, 77.03, 61.06.

(*E*)-5-Methylthiophene-2-carbaldehyde *O*-prop-2-yn-1-yl oxime (2b). Compound **2b** was synthesized according to the general procedure using (*E*)-5-methylthiophene-2-carbaldehyde oxime **1b** (277 mg, 1.96 mmol), propargyl bromide (280 mg, 2.35 mmol) and K_2CO_3 (325 mg, 2.35 mmol). After column chromatography (CH_2Cl_2 : MeOH = 100 : 1), compound **2b** was isolated as a yellow oil (314 mg, 89 %). ^{1}H-NMR (300 MHz, DMSO) *δ*/ppm: 7.86 (s, 1H, –C<u>H</u>=N–), 7.36 (d, *J* = 3.6 Hz, 1H, H-3), 6.87 (dd, *J* = 3.7, 1.3 Hz, 1H, H-4), 4.80 (d, *J* = 2.4 Hz, 2H, C<u>H</u>$_2$), 3.50 (t, *J* = 2.3 Hz, 1H, C<u>H</u>), 2.48 (s, 3H, C<u>H</u>$_3$). ^{13}C-NMR (75 MHz, DMSO) *δ*/ppm: 146.51, 141.47, 133.54, 128.11, 125.26, 80.03, 77.49, 61.49, 14.80.

(*E*)-5-Bromothiophene-2-carbaldehyde *O*-prop-2-yn-1-yl oxime (2c). Compound **2c** was synthesized according to the general procedure using (*E*)-5-bromothiophene-2-carbaldehyde oxime **1c** (315 mg, 1.53 mmol), propargyl bromide (218 mg, 1.84 mmol) and K_2CO_3 (253 mg, 1.84 mmol). After column chromatography (CH_2Cl_2 : MeOH = 100 : 1), compound **2c** was isolated as a yellow oil (60 mg,

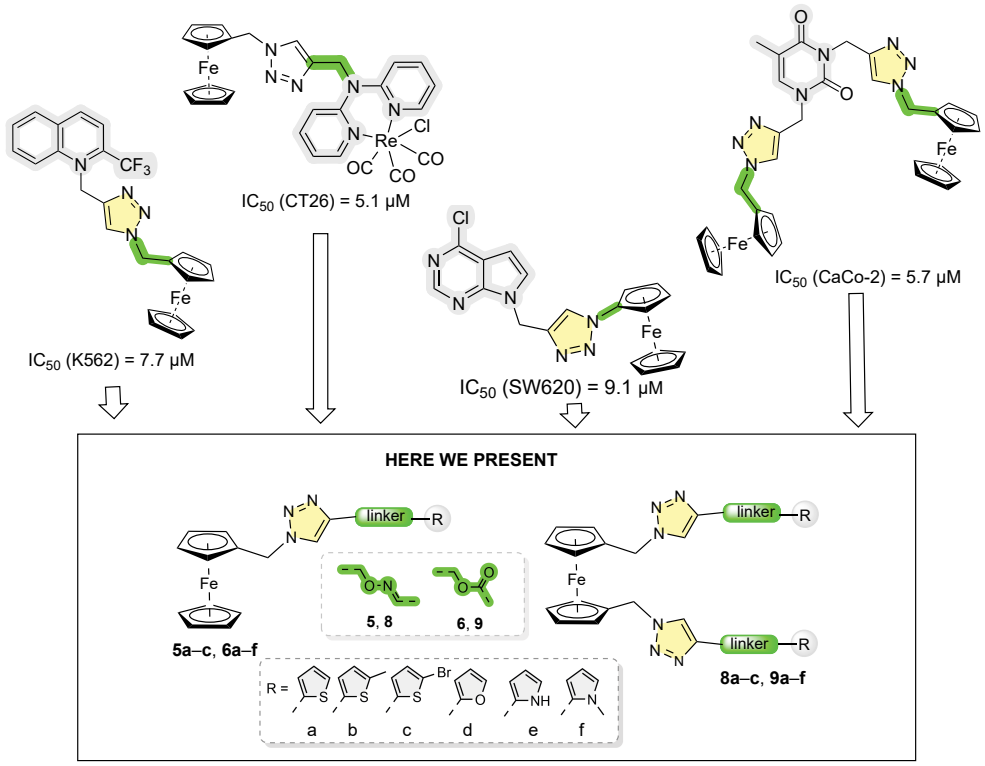


Figure 1. Design of mono- (**5a**–**c**, **6a**–**f**) and disubstituted (**8a**–**c**, **9a**–**f**) ferrocene derivatives with aldoxime ether- and ester-linked five-membered heterocycles.

16 %). ^{1}H-NMR (300 MHz, DMSO) *δ*/ppm: 7.99 (s, 1H, –CH=N–), 7.42 (d, *J* = 4.1 Hz, 1H, H-3), 7.33 (d, *J* = 3.9 Hz, 1H, H-4), 4.86 (d, *J* = 2.2 Hz, 2H, CH_2), 3.55 (t, *J* = 2.3 Hz, 1H, CH). ^{13}C-NMR (75 MHz, DMSO) *δ*/ppm:141.10, 133.55, 131.74, 129.93, 119.10, 79.68, 77.86, 61.80.

Prop-2-yn-1-yl 5-methylthiophene-2-carboxylate (3b). Compound **3b** was synthesized according to the general procedure using 5-methylthiophene-2-carboxylic acid (1 g, 7.04 mmol), propargyl bromide (997 mg, 8.45 mmol) and K_2CO_3 (1.2 g, 8.45 mmol). After extraction, compound **3b** was isolated as a colorless oil (1.25 g, 98 %). ^{1}H-NMR (600 MHz, DMSO) *δ*/ppm: 7.67 (d, *J* = 3.6 Hz, 1H, H-3), 6.96–6.95 (m, 1H, H-4), 4.89 (d, *J* = 2.5 Hz, 2H, CH_2), 3.60 (t, 1H, CH), 2.52 (s, *J* = 1.2 Hz, 3H, CH_3). ^{13}C-NMR (151 MHz, DMSO) *δ*/ppm: 160.48, 148.89, 134.71, 129.23, 127.29, 78.00, 52.32, 15.35.

Prop-2-yn-1-yl 5-bromothiophene-2-carboxylate (3c). Compound **3c** was synthesized according to the general procedure using 5-bromothiophene-2-carboxylic acid (500 mg, 2.41 mmol), propargyl bromide (345 mg, 2.90 mmol) and K_2CO_3 (400 mg, 2.90 mmol). After extraction, compound **3c** was isolated as a colorless oil (457 mg, 77 %). ^{1}H-NMR (300 MHz, DMSO) *δ*/ppm: 7.69 (d, *J* = 4.0 Hz, 1H, H-3), 7.39 (d, *J* = 4.0 Hz, 1H, H-4), 4.93 (d, *J* = 2.4 Hz, 2H, CH_2), 3.64 (t, *J* = 2.4 Hz, 1H, CH). ^{13}C-NMR (75 MHz, DMSO) *δ*/ppm: 159.48, 135.12, 133.22, 132.19, 120.43, 99.50, 78.35, 52.89.

Prop-2-yn-1-yl 1*H*-pyrrole-2-carboxylate (3e). Compound **3e** was synthesized according to the general procedure using 1*H*-pyrrole-2-carboxylic acid (500.0 mg, 4.50 mmol), propargyl bromide (643 mg, 5.40 mmol) and K_2CO_3 (746 mg, 5.40 mmol). After extraction, compound **3e** was isolated as a yellow oil (636 mg; 94 %). ^{1}H-NMR (600 MHz, DMSO) *δ*/ppm: 11.93 (s, 1H, NH), 7.07 (td, *J* = 2.7, 1.5 Hz, 1H, H-3), 6.86 (ddd, *J* = 3.8, 2.4, 1.5 Hz, 1H, H-4), 6.22 (dt, *J* = 3.7, 2.3 Hz, 1H, H-5), 4.86 (d, *J* = 2.4 Hz, 2H, CH_2), 3.49 (t, *J* = 2.4 Hz, 1H, CH). ^{13}C-NMR (151 MHz, DMSO) *δ*/ppm: 159.96, 125.28, 121.37, 116.37, 110.41, 83.75, 77.77, 51.61.

Prop-2-yn-1-yl 1-methyl-1*H*-pyrrole-2-carboxylate (3f). Compound **3f** was synthesized according to the general procedure using 1-methyl-1*H*-pyrrole-2-carboxylic acid (1.0 g, 7.99 mmol), propargyl bromide (1.1 g, 9.59 mmol) and K_2CO_3 (1.3 g, 9.59 mmol). After extraction, compound **3f** was isolated as a yellow oil (1.1 g, 84 %). ^{1}H-NMR (600 MHz, DMSO) *δ*/ppm: 7.17–7.11 (m, 1H, H-3), 6.88 (dd, *J* = 4.0, 1.8 Hz, 1H, H-4), 6.11 (dd, *J* = 4.0, 2.6 Hz, 1H, H-5), 4.83 (d, *J* = 2.5 Hz, 2H, CH_2), 3.86 (s, 3H, CH_3), 3.55 (t, *J* = 2.3 Hz, 1H, CH). ^{13}C-NMR (151 MHz, DMSO) *δ*/ppm: 162.28, 159.41, 130.98, 120.73, 117.96, 107.91, 77.46, 51.03, 36.32.

Synthesis of Monosubstituted (5a–c, 6a–f) and Disubstituted (8a–c, 9a–f) Ferrocenyl Oxime Ether- and Ester-Linked Derivatives

General Procedure for the Synthesis of Monosubstituted Ferrocenyl Aldoxime Ether- and Ester- Linked Derivatives (5a–c, 6a–f)

A mixture of the corresponding *O*-propargylated aldoximes **2a–c** or *O*-propargylated carboxylic acids **3a–f** (1.2 equiv.) and (azidomethyl)ferrocene **4** (1 equiv.) was placed in one half of the reaction vessel, while the other half was loaded with $Cu(OAc)_2$ (0.05 equiv.), methanol (30 µL), and two stainless steel balls (7 mm diameter). The components were ground under LAG mechanochemical conditions at 30 Hz for 1.5 h. The resulting crude products were purified by column chromatography on silica gel and Al_2O_3 using dichloromethane as the eluent.

(*E*)-((((((Thiophen-2-ylmethylene)amino)oxy)methyl)-1*H*-1,2,3-triazol-1-yl)methyl)ferrocene (5a). Compound **5a** was synthesized according to the general procedure using (*E*)-thiophene-2-carbaldehyde *O*-prop-2-yn-1-yl oxime **2a** (123 mg, 0.75 mmol), (azidomethyl)ferrocene **4** (150 mg, 0.62 mmol), methanol (30 µL) and $Cu(OAc)_2$ (6 mg, 0.03 mmol). After column chromatography (CH_2Cl_2 : MeOH = 50 : 1), compound **5a** was isolated as a yellow powder (229 mg, 89%, m.p. = 134–135 °C). ^{1}H-NMR (300 MHz, DMSO) *δ*/ppm: 8.16 (s, 1H, H-triazole), 7.94 (d, *J* = 0.9 Hz, 1H, –CH=N–), 7.78 (dt, *J* = 5.1, 1.1 Hz, 1H, H-5), 7.53 (dd, *J* = 3.7, 1.3 Hz, 1H, H-3), 7.14 (dd, *J* = 5.1, 3.7 Hz, 1H, H-4), 5.31 (s, 2H, CH_2), 5.26 (s, 2H, CH_2), 4.33 (t, *J* = 1.8 Hz, 2H, H-Fc), 4.17 (s, 7H, H-Fc). ^{13}C-NMR (151 MHz, DMSO) *δ*/ppm: 143.56, 141.36, 133.37, 132.87, 131.08, 127.08, 124.57, 83.05, 69.11, 69.07, 68.78, 67.87, 67.83, 49.33, 49.30. HRMS (ESI Q-TOF): Calcd. for $C_{19}H_{18}FeN_4OS$ $[M]^+$ = 407.0385; found = 407.0389.

(E)-((((((5-Methylthiophene-2-ylmethylene)amino)oxy)methyl)-1H-1,2,3-triazol-1-yl)methyl)ferrocene (5b). Compound **5b** was synthesized according to the general procedure using (*E*)-5-methylthiophene-2-carbaldehyde *O*-prop-2-yn-1-yl oxime **2b** (134 mg, 0.75 mmol), (azidomethyl)ferrocene **4** (150 mg, 0.62 mmol), methanol (30 µL) and $Cu(OAc)_2$ (5.6 mg, 0.03 mmol). After column chromatography (CH_2Cl_2 : MeOH = 50 : 1), compound **5b** was isolated as a yellow powder (195 mg, 74 **%** m.p. = 139–142 °C). ^{1}H-NMR (300 MHz, DMSO) *δ*/ppm: 8.16 (s, 1H, H-triazole), 7.80 (s, 1H, –CH=N–), 7.31 (d, *J* = 3.6 Hz, 1H, H-3), 6.83 (d, *J* = 2.8 Hz, 1H, H-4), 5.31 (s, 2H, CH_2), 5.22 (s, 2H, CH_2), 4.33 (d, *J* = 1.7 Hz, 2H, H-Fc), 4.16 (s, 7H, H-Fc), 2.42 (s, 3H, CH_3). ^{13}C-NMR (151 MHz, DMSO) *δ*/ppm: 142.50, 140.00, 139.97, 131.37, 131.35, 123.25, 123.23, 122.51, 67.16, 67.08, 66.98, 65.51, 48.19. Calcd. for $C_{20}H_{20}FeN_4OS$ $[M]^+$ = 420.0702; found = 420.0702

(*E*)-((((((5-Bromothiophene-2-ylmethylene)amino)oxy)methyl)-1*H*-1,2,3-triazol-1-yl)methyl) ferrocene (5c). Compound **5c** was synthesized according to the general procedure using (*E*)-5-bromothiophene-2-carbaldehyde *O*-prop-2-yn-1-yl oxime **2c** (182 mg, 0.75 mmol), (azidomethyl)ferrocene **4** (150 mg, 0.62 mmol), methanol (30 µL) and $Cu(OAc)_2$ (5.6 mg, 0.03 mmol). After column chromatography (CH_2Cl_2 : MeOH = 50 : 1), compound **5c** was isolated as a yellow powder (215 mg, 77 **%**, m.p. = 124–126 °C). ^{1}H NMR (400 MHz, DMSO) *δ*/ppm: 8.20 (s, 1H, H-triazole), 7.92 (s, 1H, –CH=N–), 7.36 (d, *J* = 4.1 Hz, 1H, H-3), 7.28 (d, *J* = 4.0 Hz, 1H, H-4), 5.31 (s, 2H, CH_2), 5.27 (s, 2H, CH_2), 4.32 (s, 2H, H-Fc), 4.18 – 4.15 (m, 7H, H-Fc). ^{13}C NMR (101 MHz, DMSO) *δ*/ppm: 142.72, 140.65, 133.11, 129.83, 124.26, 118.82, 82.69, 68.61, 68.46, 68.27, 67.53, 48.82. Calcd. for $C_{19}H_{17}BrFeN_4OS$ $[M]^+$ = 483.9652; found = 483.9647.

(((((Thiophene-2-carbonyl)oxy)methyl)-1*H*-1,2,3-triazol-1-yl)methyl)ferrocene (6a). Compound **6a** was synthesized according to the general procedure using prop-2-yn-1-yl thiophene-2-carboxylate **3a** (165 mg, 0.99 mmol), (azidomethyl)ferrocene **4** (200 mg, 0.83 mmol), methanol (30 µL) and $Cu(OAc)_2$ (7.5 mg, 0.04 mmol). After column chromatography (CH_2Cl_2 : MeOH = 50 : 1), compound **6a** was isolated as a yellow powder (250 mg, 74 %, m.p. = 135–137 °C). ^{1}H-NMR (300 MHz, DMSO) *δ*/ppm: 8.22 (s, 1H, H-triazole), 7.95 (dd, *J* = 4.9, 1.0 Hz, 1H, H-3), 7.80 (dd, *J* = 3.7, 1.0 Hz, 1H, H-5), 7.20 (dd, *J* = 4.8, 3.9 Hz, 1H, H-4), 5.34 (s, 2H, CH_2), 5.32 (s, 2H, CH_2), 4.37–4.33 (m, 2H, H-Fc), 4.17 (s, 7H, H-Fc). ^{13}C-NMR (75 MHz, DMSO) *δ*/ppm: 161.12, 141.55, 134.23, 134.00, 132.44, 128.40, 124.52, 82.37, 68.66, 68.59, 68.32, 57.92, 48.88. Calcd. for $C_{19}H_{17}FeN_3O_2S$ $[M]^+$ = 407.0386; found = 407.0386.

(((((5-Methylthiophene-2-carbonyl)oxy)methyl)-1*H*-1,2,3-triazol-1-yl)methyl)ferrocene (6b). Compound **6b** was synthesized according to the general procedure using prop-2-yn-1-yl 5-methylthiophene-2-carboxylate **3b** (179 mg, 0.99 mmol), (azidomethyl)ferrocene **4** (200 mg, 0.83 mmol), methanol (30 µL) and $Cu(OAc)_2$ (7.5 mg, 0.04 mmol). After column chromatography (CH_2Cl_2 : MeOH = 50 : 1), compound **6b** was isolated as a yellow powder (260 mg, 74 %, m.p. = 129–131 °C). ^{1}H-NMR (300 MHz, DMSO) *δ*/ppm: 8.19 (s, 1H, H-triazole), 7.61 (d, *J* = 3.7 Hz, 1H, H-3), 6.91 (dd, *J* = 3.6, 0.8 Hz, 1H, H-4), 5.31 (s, 2H, CH_2), 5.31 (s, 2H, CH_2), 4.37–4.33 (m, 2H, H-Fc), 4.18 (s, 7H, H-Fc), 2.48 (s, 3H, CH_3). ^{13}C-NMR (151 MHz, DMSO) *δ*/ppm: 160.99, 148.49, 141.66, 134.37, 129.77, 127.15, 124.47, 82.40, 68.702, 68.65, 68.38, 57.735, 48.90, 15.32. Calcd. for $C_{20}H_{19}FeN_3O_2S$ $[M]^+$ = 421.0542; found = 421.0542.

(((((5-Bromothiophene-2-carbonyl)oxy)methyl)-1*H*-1,2,3-triazol-1-yl)methyl)ferrocene (6c). Compound **6c** was synthesized according to the general procedure using prop-2-yn-1-yl 5-bromothiophene-2-carboxylate **3c** (244 mg, 0.99 mmol), (azidomethyl)ferrocene **4** (200 mg, 0.83 mmol), methanol (30 µL) and $Cu(OAc)_2$ (7.5 mg, 0.04 mmol). After column chromatography (CH_2Cl_2 : MeOH = 50 : 1), compound **6c** was isolated as a yellow powder (359 mg, 88 **%**, m.p. = 148–149 °C). ^{1}H-NMR (300 MHz, DMSO) *δ*/ppm: 8.22 (s, 1H, H-triazole), 7.63 (d, *J* = 4.0 Hz, 1H, H-3), 7.35 (d, *J* = 4.0 Hz, 1H, H-4), 5.34 (s, 2H, CH_2), 5.32 (s, 2H, CH_2), 4.37–4.31 (m, 1H, H-Fc), 4.17 (s, 7H, H-Fc). ^{13}C-NMR (151 MHz, DMSO) *δ*/ppm: 159.96, 141.32, 134.79, 133.75, 132.08, 124.57, 120.05, 82.35, 68.68, 68.59, 68.33, 58.28, 48.89. Calcd. for $C_{19}H_{16}BrFeN_3O_2S$ $[M]^+$ = 484.9492; found = 484.9493.

(((((Furan-2-carbonyl)oxy)methyl)-1*H*-1,2,3-triazol-1-yl)methyl)ferrocene (6d). Compound **6d** was synthesized according to the general procedure using prop-2-yn-1-yl furan-2-carboxylate **3d** (74 mg, 0.49 mmol), (azidomethyl)ferrocene **4** (100 mg, 0.41 mmol), methanol (30 µL), and $Cu(OAc)_2$ (3.7 mg, 0.02 mmol). After column chromatography (CH_2Cl_2 : MeOH = 50 : 1), compound **6d** was isolated as a yellow powder (117 mg, 73 **%**, m.p. = 141–143 °C). ^{1}H-NMR (300 MHz, DMSO) *δ*/ppm: 8.20 (s, 1H, H-triazole), 7.96 (d, *J* = 0.8 Hz, 1H, H-5), 7.30 (d, *J* = 3.4 Hz, 1H, H-3), 6.67 (dd, *J* = 3.5, 1.7 Hz, 1H, H-4), 5.33 (s, 2H, CH_2), 5.32 (s, 2H, CH_2), 4.45–4.26 (m, 2H, H-Fc), 4.18 (s, 7H, H-Fc). ^{13}C-NMR (151 MHz, DMSO) *δ*/ppm: 157.52, 147.82, 143.42, 141.46, 124.52, 118.76, 112.34, 82.29, 68.69, 68.60, 68.34, 57.53, 48.91. Calcd. for $C_{19}H_{17}FeN_3O_3$ $[M]^+$ = 391.0614; found = 391.0615.

(((((Pyrrole-carbonyl)oxy)methyl)-1*H*-1,2,3-triazol-1-yl)methyl)ferrocene (6e). Compound **6e** was synthesized according to the general procedure using prop-2-yn-1-yl 1*H*-pyrrole-2-carboxylate **3e** (73 mg, 0.50 mmol), (azidomethyl)ferrocene **4** (100 mg, 0.42 mmol), methanol (30 µL) and $Cu(OAc)_2$ (3.7 mg, 0.02 mmol). After column chromatography (CH_2Cl_2 : MeOH = 50 : 1), compound **6e** was isolated as a yellow powder (115 mg, 73 **%**, m.p. = 142–144 °C). ^{1}H-NMR (300 MHz, DMSO) *δ*/ppm: 11.90 (s, 1H, NH), 8.16 (s, 1H, H-triazole), 7.00 (d, *J* = 1.2 Hz, 1H, H-3), 6.76 (s, 1H, H-4), 6.27–5.97 (m, 1H, H-5), 5.31 (s, 2H, CH_2), 5.27 (s, 2H, CH_2), 4.36–4.32 (m, 2H, H-Fc), 4.18 (s, 7H, H-Fc). ^{13}C-NMR (75 MHz, DMSO) *δ*/ppm: 159.96, 142.14, 124.34, 124.23, 121.36, 115.45, 109.60, 82.29, 68.70, 68.60, 68.34, 56.71, 48.88. Calcd. for $C_{19}H_{18}FeN_4O_2$ $[M]^+$ = 390.0774; found = 390.0774.

(((((1-Methyl-1*H*-pyrrole)oxy)methyl)-1*H*-1,2,3-triazol-1-yl)methyl)ferrocene (6f). Compound **6f** was synthesized according to the general procedure using prop-2-yn-1-yl 1-methyl-1*H*-pyrrole-2-carboxylate **3f** (162 mg, 0.99 mmol), (azidomethyl)ferrocene **4** (200 mg, 0.83 mmol), methanol

(30 µL) and $Cu(OAc)_2$ (7.5 mg, 0.04 mmol). After column chromatography (CH_2Cl_2 : MeOH = 50 : 1), compound **6f** was isolated as a yellow powder (275 mg, 82 **%**, m.p. = 121–123 °C). ^{1}H-NMR (300 MHz, DMSO) δ/ppm: 8.18 (s, 1H, H-triazole), 7.12–7.06 (m, 1H, H-5), 6.80 (dd, J = 4.0, 1.9 Hz, 1H, H-4), 6.06 (dd, J = 4.1, 2.4 Hz, 1H, H-3), 5.31 (s, 2H, CH_2), 5.26 (s, 2H, CH_2), 4.37–4.32 (m, 2H, H-Fc), 4.18 (d, J = 3.4 Hz, 7H, H-Fc), 3.84 (s, 3H, CH_3).^{13}C-NMR (151 MHz, DMSO) δ/ppm: 159.97, 142.15, 130.62, 124.22, 121.16, 117.69, 107.72, 82.45, 68.64, 68.58, 68.29, 56.63, 48.84, 36.31 Calcd. for $C_{20}H_{20}FeN_4O_2$ $[M]^+$ = 404.0930; found = 404.0931.

General Procedure for the Synthesis of Disubstituted Ferrocenyl Aldoxime Ether- and Ester-Linked Derivatives (8a–c, 9a–f)

A mixture of the corresponding *O*-propargylated aldoximes **2a**–**c** or *O*-propargylated carboxylic acids **3a**–**f** (2.4 equiv.) and 1,1′-bis(azidomethyl)ferrocene **7** (1 equiv.) was placed in one half of the reaction vessel, while the other half was loaded with $Cu(OAc)_2$ (0.1 equiv.), methanol (30 µL) and two stainless steel balls (7 mm diameter). The components were ground under LAG mechanochemical conditions at 30 Hz for 1.5 h. The resulting crude products were purified by column chromatography on silica gel and Al_2O_3 using dichloromethane as the eluent.

1,1'-Bis((4-(((((*E*)-thiophen-2-ylmethylene)amino)oxy)methyl)-1*H*-1,2,3-triazol-1-yl)methyl)ferrocene) (8a). Compound **8a** was synthesized according to the general procedure using thiophene-2-carbaldehyde *O*-prop-2-yn-1-yl oxime **2a** (67 mg, 0.41 mmol), 1,1'-bis(azidomethyl)ferrocene **7** (50 mg, 0.17 mmol), methanol (30 µL) and $Cu(OAc)_2$ (3.1 mg, 0.02 mmol). After column chromatography (CH_2Cl_2 : MeOH = 50 : 1), compound **8a** was isolated as yellow powder (50 mg, 47 **%**, m.p. = 130–132 °C). ^{1}H-NMR (300 MHz, DMSO) δ/ppm: 8.14 (s, 2H, H-triazole), 7.93 (s, 2H, –CH=N–), 7.77 (d, J = 5.1 Hz, 2H, H-5), 7.52 (d, J = 3.0 Hz, 2H, H-3), 7.13 (dd, J = 4.9, 3.8 Hz, 2H, H-4), 5.32 (s, 4H, CH_2), 5.26 (s, 4H, CH_2), 4.33 (s, 4H, H-Fc), 4.17 (s, 4H, H-Fc). ^{13}C-NMR (75 MHz, DMSO) δ/ppm: 143.07, 140.84, 132.85, 132.35, 130.55, 126.56, 124.02, 83.12, 69.47, 69.22, 67.35, 48.55. Calcd. for $C_{28}H_{26}FeN_8O_2S_2$ $[M]^+$ = 626.0964; found = 626.0965.

1,1'-Bis((4-(((((*E*)-(5-methylthiophen-2-yl)methylene)amino)oxy)methyl)-1*H*-1,2,3-triazol-1-yl)methyl)ferrocene (8b). Compound **8b** was synthesized according to the general procedure using (*E*)-5-methylthiophene-2-carbaldehyde *O*-prop-2-yn-1-yl oxime **2b** (73 mg, 0.41 mmol), 1,1'-bis(azidomethyl)ferrocene **7** (50 mg, 0.17 mmol), methanol (30 µL) and $Cu(OAc)_2$ (3.1 mg, 0.02 mmol). After column chromatography (CH_2Cl_2 : MeOH = 50 :1), compound **8b** was isolated as yellow powder (65 mg, 59 **%**, m.p. = 150–152 °C). ^{1}H-NMR (300 MHz, DMSO) δ/ppm 8.14 (s, 2H, H-triazole), 7.80 (s, 2H, –CH=N–), 7.31 (d, J = 3.6 Hz, 2H, H-3), 6.82 (dd, J = 3.6, 0.9 Hz, 2H, H-4), 5.32 (s, 4H, CH_2), 5.22 (s, 4H, CH_2), 4.44–4.28 (m, 4H, H-Fc), 4.25–4.10 (m, 4H, H-Fc), 2.41 (s, 6H, CH_3) ^{13}C-NMR (151 MHz, DMSO) δ/ppm 146.11, 143.11, 140.98, 133.10, 128.62, 125.15, 123.98, 83.18, 69.50, 69.20, 67.25, 48.51, 14.77. Calcd. for $C_{30}H_{30}FeN_8O_2S_2$ $[M]^+$ = 654.1278; found = 654.1279.

3,4-Bis((4-(((((*E*)-(5-bromothiophen-2-yl)methylene)amino)oxy)methyl)-1*H*-1,2,3-triazol-1-yl)methyl)ferrocene (8c). Compound **8c** was synthesized according to the general procedure using (*E*)-5-bromothiophene-2-carbaldehyde *O*-prop-2-yn-1-yl oxime **2c** (98 mg, 0.41 mmol), 1,1'-bis(azidomethyl)ferrocene **7** (50 mg, 0.17 mmol), methanol (30 µL) and $Cu(OAc)_2$ (3.1 mg, 0.02 mmol). After column chromatography (CH_2Cl_2 : MeOH = 50 : 1), compound **8c** was isolated as yellow powder (26 mg, 20 **%** m.p. = 178–180 °C). ^{1}H NMR (300 MHz, DMSO) δ/ppm: 8.17 (s, 2H, H-triazole), 7.92 (s, 2H, –CH=N–), 7.35 (d, J = 4.1 Hz, 2H, H-3), 7.27 (d, J = 4.0 Hz, 2H, H-4), 5.33 (s, 4H, CH_2), 5.27 (s, 4H, CH_2), 4.33–4.32 (m, 4H, H-Fc), 4.17–4.15 (m, 4H, H-Fc). ^{13}C NMR (75 MHz, DMSO) δ/ppm: 142.77, 140.63, 133.08, 131.88, 129.79, 124.18, 118.81, 83.19, 69.40, 69.22, 67.50, 48.56. Calcd. for $C_{28}H_{24}Br_2FeN_8O_2S_2$ $[M]^+$ = 783.9156; found = 783.9158.

1,1'-Bis((4-(((thiophene-2-carbonyl)oxy)methyl)-1*H*-1,2,3-triazol-1-yl)methyl)ferrocene (9a). Compound **9a** was synthesized according to the general procedure using prop-2-yn-1-yl thiophene-2-carboxylate **3a** (134 mg, 0.81 mmol), 1,1'-bis(azidomethyl)ferrocene **7** (100 mg, 0.34 mmol), methanol (30 µL) and $Cu(OAc)_2$ (6.1 mg, 0.03 mmol). After column chromatography (CH_2Cl_2 : MeOH = 30 : 1), compound **9a** was isolated as a yellow powder (95 mg, 44 **%**, m.p. = 73–74°C). ^{1}H-NMR (300 MHz, DMSO) δ/ppm: 8.21 (s, 2H, H-triazole), 7.94 (dd, J = 4.9, 1.1 Hz, 2H, H-3), 7.79 (dd, J = 3.7, 1.1 Hz, 2H, H-4), 7.19 (dd, J = 4.9, 3.8 Hz, 2H, H-5), 5.40–5.22 (m, 8H, CH_2), 4.37–4.34 (m, 4H, H-Fc), 4.22–4.13 (m, 4H, H-Fc). ^{13}C-NMR (75 MHz, DMSO) δ/ppm: 161.10, 141.66, 134.22, 133.99, 132.40, 128.38, 124.57, 82.94, 69.56, 69.26, 57.91, 48.60. Calcd. for $C_{28}H_{28}FeN_8O_2S_2$ $[M+Na]^+$ = 651.0543; found = 651.0543.

1,1'-Bis((4-(((5-methylthiophene-2-carbonyl)oxy)methyl)-1*H*-1,2,3-triazol-1-yl)methyl)ferrocene (9b) Compound **9b** was synthesized according to the general procedure using prop-2-yn-1-yl 5-methylthiophene-2-carboxylate **3b** (73 mg, 0.41 mmol), 1,1'-bis(azidomethyl)ferrocene **7** (50 mg, 0.17 mmol), methanol (30 µL) and $Cu(OAc)_2$

(3.1 mg, 0.02 mmol). After column chromatography (CH_2Cl_2 : MeOH = 30 : 1), compound **9b** was isolated as a yellow powder (51 mg, 46 **%**, m.p. = 159–160 °C). ^{1}H-NMR (300 MHz, DMSO) *δ*/ppm: 8.18 (s, 2H, H-triazole), 7.60 (d, *J* = 3.7 Hz, 2H, H-3), 6.90 (d, *J* = 3.0 Hz, 2H, H-4), 5.33 (s, 4H, CH_2), 5.31 (s, 4H, CH_2), 4.36 (s, 4H, H-Fc), 4.19 (s, 4H, H-Fc), 2.48 (s, 6H, CH_3). ^{13}C-NMR (151 MHz, DMSO) *δ*/ppm: 160.97, 148.48, 141.69, 134.36, 129.74, 127.13, 124.45, 82.97, 69.58, 69.28, 57.73, 48.62, 15.30. Calcd. for $C_{30}H_{28}FeN_6O_4S_2$ $[M+Na]^+$ = 679.0856; found = 679.0856.

1,1'-Bis((4-(((5-bromothiophene-2-carbonyl)oxy)methyl)-1*H*-1,2,3-triazol-1-yl)methyl) ferrocene (9c). Compound **9c** was synthesized according to the general procedure using prop-2-yn-1-yl 5-bromothiophene-2-carboxylate **3c** (99 mg, 0.41 mmol), 1,1'-bis(azidomethyl)ferrocene **7** (50 mg, 0.17 mmol), methanol (30 µL) and $Cu(OAc)_2$ (3 mg, 0.02 mmol). After column chromatography (CH_2Cl_2 : MeOH = 30 : 1), compound **9c** was isolated as a yellow powder (86 mg, 65 **%**, m.p. = 170–172 °C). ^{1}H-NMR (300 MHz, DMSO) *δ*/ppm: 8.21 (s, 2H, H-triazole), 7.62 (d, *J* = 4.0 Hz, 2H, H-3), 7.34 (d, *J* = 4.0 Hz, 2H, H-4), 5.34 (s, 4H, CH_2), 5.33 (s, 4H, CH_2), 4.36 (s, 4H, H-Fc), 4.19 (s, 4H, H-Fc). ^{13}C-NMR (75 MHz, DMSO) *δ*/ppm: 159.90, 141.36, 134.76, 133.73, 132.05, 124.54, 120.03, 82.94, 69.56, 69.26, 58.26, 48.61. Calcd. for $C_{28}H_{22}Br_2FeN_6O_4S_2$ $[M+Na]^+$ = 808.8735; found = 808.8732.

1,1'-Bis((4-(((furan-2-carbonyl)oxy)methyl)-1*H*-1,2,3-triazol-1-yl)methyl)ferrocene (9d). Compound **9d** was synthesized according to the general procedure using prop-2-yn-1-yl furan-2-carboxylate **3d** (61 mg, 0.41 mmol), 1,1'-bis(azidomethyl)ferrocene **7** (50 mg, 0.17 mmol), methanol (30 µL) and $Cu(OAc)_2$ (3.1 mg, 0.02 mmol). After column chromatography (CH_2Cl_2 : MeOH = 30 : 1), compound **9d** was isolated as a yellow powder (32 mg, 32 **%** m.p. = 105–106 °C). ^{1}H-NMR (300 MHz, DMSO) *δ*/ppm: 8.19 (s, 2H, H-triazole), 7.95 (dd, *J* = 1.7, 0.7 Hz, 2H, CH), 7.29 (dd, *J* = 3.5, 0.7 Hz, 2H, CH), 6.67 (dd, *J* = 3.5, 1.7 Hz, 2H, CH), 5.34 (s, 4H, CH_2), 5.33 (s, 4H, CH_2), 4.37 (pt, 4H, H-Fc), 4.20 (pt, 4H, H-Fc). ^{13}C-NMR (75 MHz, DMSO) *δ*/ppm: 157.54, 147.82, 143.41, 141.52, 124.53, 118.79, 112.35, 82.92, 69.61, 69.31, 57.53, 48.65. Calcd. for $C_{28}H_{24}FeN_6O_6$ $[M+Na]^+$ = 619.0999; found = 619.0999.

1,1'-Bis((4-(((1*H*-pyrrole-2-carbonyl)oxy)methyl)-1*H*-1,2,3-triazol-1-yl)methyl)ferrocene (9e). Compound **9e** was synthesized according to the general procedure using prop-2-yn-1-yl 1*H*-pyrrole-2-carboxylate **3e** (60 mg, 0.41 mmol), 1,1'-bis(azidomethyl)ferrocene **7** (50 mg, 0.17 mmol), methanol (30 µL) and $Cu(OAc)_2$ (1 mg, 0.03 mmol). After column chromatography (CH_2Cl_2 : MeOH = 30 : 1), compound **9e** was isolated as a yellow powder (37 mg, 37 **%**, m.p. = 178–179 °C). ^{1}H-NMR (300 MHz, DMSO) *δ*/ppm: 11.89 (s, 2H, NH), 8.15 (s, 2H, H-triazole), 7.00 (dd, *J* = 4.2, 2.7 Hz, 2H, H-3), 6.84–6.48 (m, 2H, H-5), 6.14 (dt, *J* = 3.7, 2.3 Hz, 2H, H-4), 5.34 (s, 4H, CH_2), 5.28 (s, 4H, CH_2), 4.37 (pt, 4H, H-Fc), 4.20 (pt, 4H, H-Fc). ^{13}C-NMR (75 MHz, DMSO) *δ*/ppm: 159.96, 142.19, 124.35, 124.22, 121.36, 115.46, 109.61, 82.90, 69.62, 69.31, 56.71, 48.62. Calcd. for $C_{28}H_{26}FeN_8O_4$ $[M]^+$ = 594.1421; found = 594.1421.

1,1'-Bis((4-(((1-methyl-1*H*-pyrrole-2-carbonyl)oxy)methyl)-1*H*-1,2,3-triazol-1-yl)methyl)ferrocene (9f). Compound **9f** was synthesized according to the general procedure using prop-2-yn-1-yl 1-methyl-1*H*-pyrrole-2-carboxylate **3f** (132 mg, 0.81 mmol), 1,1'-bis(azidomethyl)ferrocene **7** (100 mg, 0.34 mmol), methanol (30 µL) and $Cu(OAc)_2$ (6.1 mg, 0.03 mmol). After column chromatography (CH_2Cl_2 : MeOH = 30 : 1), compound **9f** was isolated as a yellow powder (92 mg, 44 **%** m.p. = 162–164 °C). ^{1}H-NMR (300 MHz, DMSO) *δ*/ppm: 8.17 (s, 2H, H-triazole), 7.09 (m, 2H, H-5), 6.80 (dd, *J* = 3.8, 1.7 Hz, 2H, H-3), 6.06 (dd, *J* = 3.8, 2.6 Hz, 2H, H-4), 5.32 (s, 4H, CH_2), 5.26 (s, 4H, CH_2), 4.35 (s, 4H, H-Fc), 4.18 (s, 4H, H-Fc), 3.83 (s, 6H, CH_3). ^{13}C-NMR (151 MHz, DMSO) *δ*/ppm: 159.98, 142.21, 130.63, 124.20, 121.14, 117.70, 107.73, 83.03, 69.55, 69.25, 56.62, 48.59, 36.31. Calcd. for $C_{30}H_{30}FeN_8O_4$ $[M]^+$ = 622.1734; found = 622.1736.

X-Ray Crystal Structure Studies

Single crystals of **5b**, **6c**, **6d**, and **6f** suitable for diffraction experiment were grown by evaporation of their nearly saturated methanol solutions. X-ray data for all crystals were collected at 297 K on a Rigaku XtaLAB Synergy-S diffractometers equipped with a HyPix-6000HE detector using mirror-monochromatized CuK_α radiation (*λ* = 1.54184 Å). All details about data collection and reduction, as well as structure solution and refinement are given in the Supporting Information. CCDC 2527731-2527734 contain the supplementary crystallographic data for this paper. These data can be obtained free of charge from the Cambridge Crystallographic Data Centre via www.ccdc.cam.ac.uk/structures.

In Vitro Antiproliferative Activity Assessment

Cell Culture and Proliferation Assays

Human tumor cell lines, non-small cell lung cancer (H460), metastatic colorectal adenocarcinoma (SW620), hepatocellular carcinoma (HepG2), and breast cancer (MCF-7), as well as normal human embryonic kidney cells (HEK293T), were obtained from the American Type Culture Collection (ATCC). Cells were cultured as adherent monolayers in Dulbecco's Modified Eagle Medium (DMEM), supplemented with 10 % fetal bovine serum (FBS), 2 mM

L-glutamine, 100 U/mL penicillin, and 100 µg/mL streptomycin. Cultures were maintained at 37 °C in a humidified atmosphere containing 5 % CO_2. For proliferation assays, cells were seeded into 96-well microtiter plates at densities of 1.5×10^4 cells/mL, except for MCF-7 cells, which were seeded at 2×10^4 cells/mL to account for their specific doubling times. Test compounds were prepared in growth medium at concentrations ranging from 10^{-8} to 10^{-4} M, using serial 10-fold dilutions, and added to the wells. The final concentration of the solvent did not exceed 0.5 %. Cells were incubated with the compounds for 72 h. Following incubation, cell proliferation was assessed using the MTT assay, which measures the reduction of the tetrazolium dye MTT to an insoluble formazan product by metabolically active cells.[51] The culture medium was removed, and 40 µL of MTT reagent (0.5 mg/mL) was added to each well. After a 4-hour incubation period, the resulting formazan crystals were solubilized by adding 160 µL of dimethyl sulfoxide (DMSO) to each well. Absorbance was measured at 570 nm using a microplate reader, with the absorbance directly correlating to cell viability. Each test condition was performed in quadruplicate across at least two independent experiments. The concentration required to inhibit cell growth by 50 % (IC_{50}) was determined from dose–response curves using linear regression analysis, interpolating concentrations that yielded percentage growth values above and below 50 %.

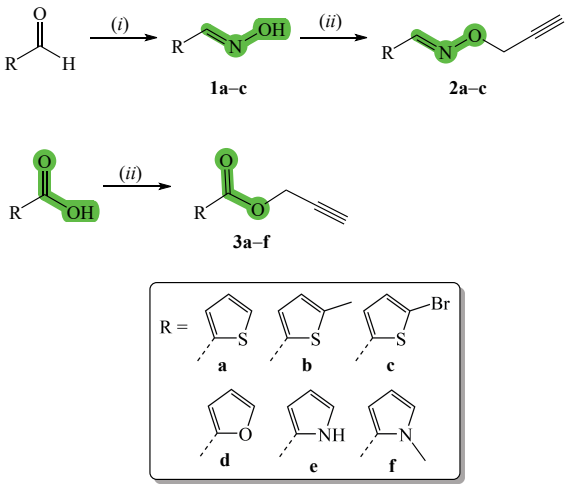
Voltammetry Measurements

Stock standard solutions of compounds **8a**, **8b**, **9c**, and **9f** ($c \approx 1 \times 10^{-2}$ M) were prepared by dissolving the appropriate amount of each solid in DMSO. Voltammetric measurements were carried out using the computer-controlled electrochemical system "PGSTAT 101" (Eco Chemie, Utrecht, The Netherlands), controlled using the electrochemical software "NOVA 1.15". All electrochemical experiments were carried out in acetonitrile containing 0.1 M tetraethylammonium perchlorate (TEAP) as the supporting electrolyte. Cyclic voltammetry (CV) measurements were performed over a potential range of 0 to 1.4 V using a glassy carbon working electrode. An Ag/Ag^+ electrode (0.01 M $AgNO_3$ in acetonitrile) was used as the reference electrode, and a platinum wire served as the auxiliary electrode. All potentials were expressed versus the Ag/Ag^+ (0.01 M $AgNO_3$) reference electrode. Before each run, the glassy carbon working electrode was polished with diamond suspension in spray (grain size 6 µm) and rinsed with ethanol and deionized water. The supporting electrolyte (0.1 M TEAP in acetonitrile) was placed in the electrochemical cell, and the required aliquot of the standard analyte solution was added. Before each experiment, the solution in the electrochemical cell was first degassed with high-purity nitrogen for 5 min, and the nitrogen blanket was maintained thereafter. All experiments were conducted at room temperature. The reported oxidation potential values represent the mean of four independent measurements.

RESULTS AND DISCUSSION

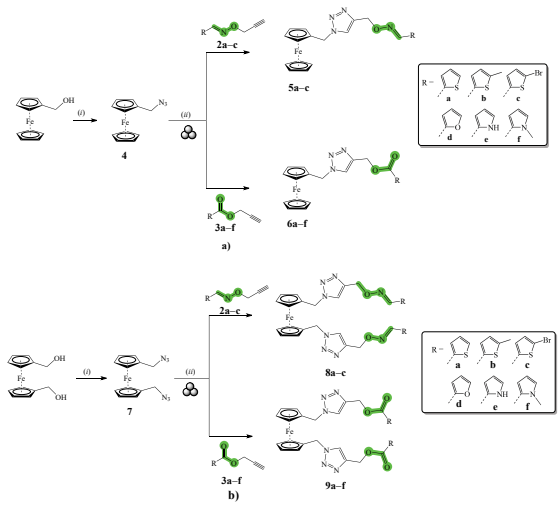
Chemistry

The targeted mono- and disubstituted ferrocene derivatives, with aldoxime ether- (**5a–c**, **8a–c**) and ester-linked (**6a–f**, **9a–f**) five-membered heterocycles, were synthesized using the efficient procedures described in Schemes 1 and 2. In the first step of the synthesis, the aldoxime derivatives **1a–c** were formed via an addition-elimination mechanism, which was catalyzed by hydroxylamine hydrochloride.[52,53] In all thiophene aldoximes, the *E*-isomer was consistently identified as the predominant product and was then subjected to the synthesis of *O*-propargylated aldoximes **2a–c**. Although furan aldoxime, pyrrole aldoxime, and *N*-methylpyrrole aldoxime were successfully synthesized and their isomers separated, *O*-alkylation of these aldoximes isolated under various conditions only traces of their *O*-propargylated aldoximes. The terminal alkynes required for the 1,3-dipolar cycloaddition were also synthesized by *O*-alkylation of the carboxylic acids **3a–f** with propargyl bromide and K_2CO_3 as a base. Ferrocene azides (**4**, **7**) were synthesized by nucleophilic substitution of the corresponding hydroxyl derivatives with sodium azide (NaN_3) in acetic acid according to methods described in the literature.[40,44]



Scheme 1. Synthesis of alkynyl derivatives **2a–c** and **3a–f**. *Reagents and conditions:* (*i*) $CH_3OH : H_2O = 8 : 1$, $NH_2OH \times HCl$, r.t, 6–12 h; (*ii*) propargyl bromide, DMF, K_2CO_3, r.t, 24 h.

The targeted mono- (**5a–c**, **6a–f**) and disubstituted (**8a–c**, **9a–f**) ferrocene derivatives, featuring ester and aldoxime ether functionalized five-membered heterocycles, were synthesized by Cu(I)-catalyzed 1,3-dipolar cycloaddition of the corresponding ferrocene azides (**4**, **7**) and *O*-propargylated heterocyclic derivatives (**2a–c**, **3a–f**). This reaction was performed via solid-state mechanochemistry under liquid-assisted grinding (LAG) conditions, as it was found that the addition of a minimal amount of solvent enhances reactivity.[54]



Scheme 2. Liquid-assisted grinding (LAG) in the synthesis of mono- **5a–c**, **6a–f** (a) and disubstituted **8a–c**, **9a–f** (b) ferrocene–heterocycle hybrids. *Reagents and conditions:* (*i*) NaN_3, CH_3COOH, 3 h, 50 °C. (*ii*) $Cu(OAc)_2$, two stainless-steel milling balls (7 mm), stainless steel vessel, methanol (30 μL), 90 min, 30 Hz.

The monosubstituted derivatives were obtained in high yields (73–89 %), while the disubstituted derivatives exhibited significantly lower yields (20–65 %) due to the formation of monosubstituted byproducts. Structural elucidation was performed by NMR spectroscopy, mass spectrometry and single crystal X-ray diffraction.

X-Ray Crystal Structure Studies

In a wish to confirm molecular structures of synthesized compounds, and to explore their conformation and supramolecular architectures, single crystal X-ray studies were carried out. We succeeded to obtain single crystals of four monosubstituted ferrocene–heterocycle hybrids. In three of them, the ester group links triazole and heterocyclic rings (**6c**, **6d** and **6f**), while in one aldoxime ether is linker (**5b**) (Figure 2). Conformation of cyclopentadienyl (Cp) rings ranges from nearly eclipsed in **6d** to halfway between eclipsed and staggered in **5b**, with mean values of the pseudo-torsion C–*Cg*–*Cg*–C angles of ca. 3° in **6d** and 18° in **5b**. In **6c**, Cp rings deviate from eclipsed

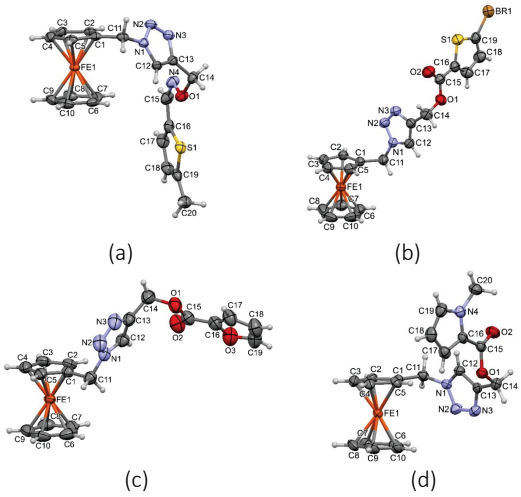


Figure 2. Molecular structures of **5b** (a), **6c** (b), **6d** (c), and **6f** (d) with atom-numbering schemes. Displacement ellipsoids for non-hydrogen atoms are drawn at the 40 % probability level.

conformation for ca. 6°, while in the case of **6f** the Cp rings are mutually rotated for ca. 11°. Conformation of C1–C5 Cp ring pendant moiety in these molecules differ significantly. Compared to **6c**, in which whole moiety is disposed almost in the same direction, pendant moieties in **5b, 6d**, and **6f** have completely different orientation (Figure 2). Thus, the C12–C13–C14–O1 and C13–C14–O1–C15 or C13–C14–O1–N4 torsion angle values show that conformation range from ±synclinal to anticlinal (Table S2, Supporting Information). Difference in conformation is the most pronounced in **5b** and **6f**, in which moieties are highly bent. It is interesting to note that thiophene, triazole and C1–C5 Cp rings in **6c** are almost perpendicular to each other and that all dihedral angles are approximately equal (Table S3, Supporting Information). On the other side, thiophene and C1–C5 Cp rings in **5b** are almost perpendicular to each other, while thiophene and triazole rings are inclined for ca. 59°.

As expected, due to the presence of aromatic rings, these structures besides C–H···O and C–H···N hydrogen bonds also comprise C–H···π and π···π interactions (Tables S4 and S5, Supporting information). In **6c**, one C–H···N and two C–H···O hydrogen bonds (Figure S44, Supporting Information) self-assemble the molecules into two-dimensional network. One π···π interaction between thiophene rings of neighboring molecules (Figure S44b, Supporting Information) also participate in supramolecular aggregation, but within the already mentioned hydrogen-bonding network (Figure 3a).

Three C–H···N hydrogen bonds and one C–H···O hydrogen bond link the molecules of **6d**, and form a two-dimensional network, very similar to that of **6c** (Figure S45,

Supporting information). Identically as in **6c**, additional supramolecular interactions, two C–H···π and two π···π, interconnect molecules within two-dimensional network. In **6f**, only C–H···N hydrogen bonds are present, and they form a one-dimensional chain motif (Figure S46, Supporting Information). Molecules are additionally bound by one C–H···π interaction, in which pyrrole ring is involved, and one π···π interaction between C1–C5 Cp rings of neighboring molecules. These two interactions assemble one-dimensional chains into three-dimensional network (Figure 3b). Interestingly, intermolecular hydrogen bonds in **5b** are absent, but there are three C–H···π interactions that form a two-dimensional network (Figure S47, Supporting Information). Two π···π interactions between triazole and C1–C5 Cp rings of mutually parallel networks built three-dimensional network, so forming, as in **6f**, higher order supramolecular structure (Figure 3c).

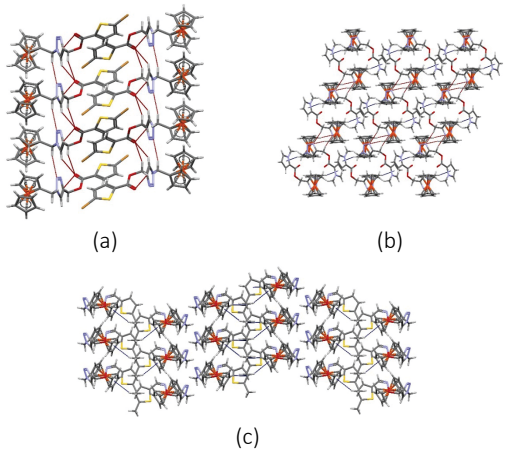


Figure 3. Partial view of molecular packing of three ferrocene–heterocycle hybrids, showing intermolecular interactions that form a two-dimensional network in **6c** (a), and three-dimensional networks in **6f** (b) and **5b** (c).

Antiproliferative Activity

The cytotoxic activity of mono- (**5a–c**, **6a–f**) and disubstituted (**8a–c, 9a–f**) triazole derivatives was tested *in vitro* on four human tumor cell lines: non-small lung cancer (H460), metastatic colorectal adenocarcinoma (SW620), hepatocellular carcinoma (HepG2), breast cancer (MCF-7) as well as on normal human embryonic kidney cells (HEK293T). The results of monosubstituted and disubstituted derivatives are presented in Tables 1 and 2, respectively.

The synthesized compounds were designed to investigate the impact of the number of triazolyl groups and various linkers and heterocyclic rings on antiproliferative activity. Overall, disubstituted ferrocene derivatives (**8a–c**, **9a–f**) demonstrated enhanced antiproliferative effects on hepatocellular carcinoma HepG2, and breast cancer MCF-7 compared to their monosubstituted counterparts (**5a–c**, **6a–f**) (Figure 4).

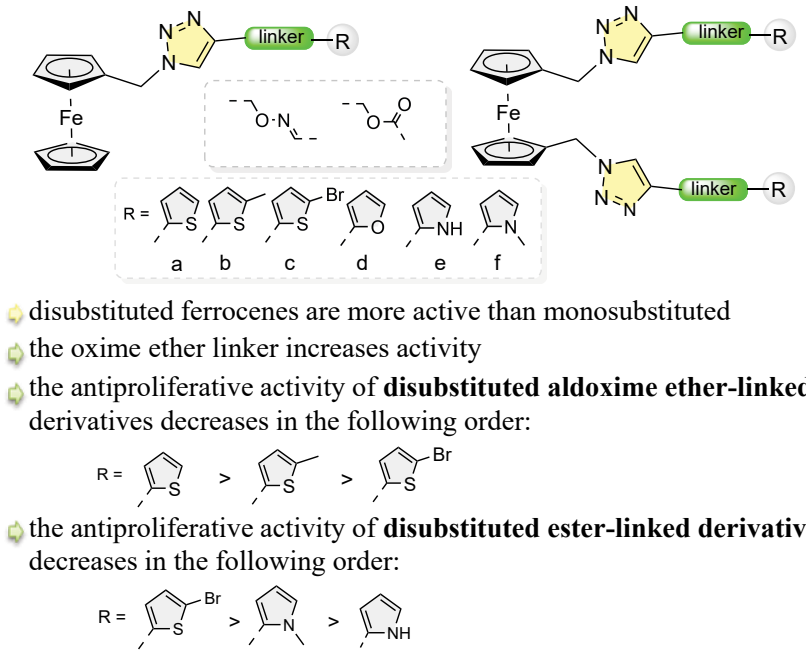
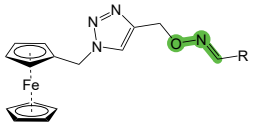
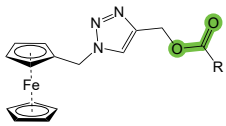


Figure 4. Structure–activity relationship analysis of mono- and disubstituted ferrocene derivatives with aldoxime ether- or ester-linked five-membered heterocycles on HepG2 and MCF-7 cells.

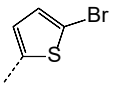
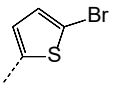
Table 1. Antiproliferative activity of monosubstituted ferrocene derivatives bearing aldoxime ether- (**5a**–**c**) and ester-linked (**6a**–**f**) five-membered heterocycles.



5a–c



6a–f

Compd	R	IC_{50}[(a)] (μM)				
		H460	SW620	HepG2	MCF-7	HEK293T
5a		>100	>100	67 ± 34	42 ± 16	84 ± 15
5b		34 ± 4	33 ± 1	24 ± 5	20 ± 1	23 ± 7
5c		41 ± 5	35 ± 10	25 ± 16	16 ± 4	22 ± 7
6a		>100	77 ± 24	84 ± 16	44 ± 10	70 ± 4
6b		>100	>100	40 ± 9	27 ± 10	57 ± 41
6c		>100	>100	>100	59 ± 40	>100
6d		>100	86 ± 15	90 ± 13	33 ± 0.1	44±0.1
6e		40 ± 1	36 ± 4	24 ± 4	18 ± 2	20 ± 8
6f		42 ± 5	52 ± 21	22 ± 7	18 ± 1	17 ± 10

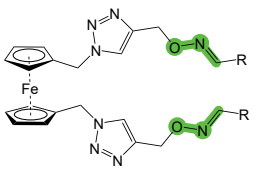
[(a)] IC_{50}; the concentration that causes 50 % growth inhibition.

Among the monosubstituted compounds, those with ester linkers (**6a**–**f**) showed moderate activity. From this series, compound **6f** containing *N*-methylpyrrole substituent was the most active, with IC_{50} values between 18 μM and 52 μM for all tested cancer cell lines. However, this compound was also toxic to normal human embryonic kidney cells HEK293T. Replacing the ester linker with an aldoxime ether enhanced antiproliferative activity. Compound **5c**, which contains a 5-bromothiophene moiety, demonstrated the highest potency against MCF-7 cells (IC_{50} = 16 μM, SI = 1.4), followed by 5-methylthiophene substituent compound **5b**, which showed slightly weaker growth-inhibition effect (IC_{50} = 20 μM, SI = 1.2).

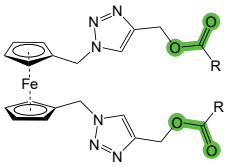
Among the aldoxime ether-linked disubstituted derivatives (**8a**–**c**), compound **8a**, with a thiophene substituent, showed strong but non-selective inhibition of HepG2 and MCF-7 cells (IC_{50} = 5 μM, SI = 1.4). Compound **8b** with 5-methylthiophene also exhibited good activity against HepG2 (IC_{50} = 6 μM) with moderate selectivity to normal cells (SI = 5.5). In contrast, 5-bromothiophene derivative **8c** showed reduced activity.

In the ester-linked disubstituted series (**9a**–**f**), compound **9f** emerged as the most promising derivative with potent and selective inhibition of HepG2 cells (IC_{50} = 5 μM), with minimal cytotoxicity toward normal cells (SI > 20). Compound **9c**, which contains a 5-bromothiophene ring, showed slightly better activity (IC_{50} = 4 μM) but lower selectivity (SI = 3.3).

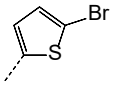
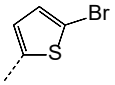
Table 2. Antiproliferative activity of disubstituted ferrocene derivatives bearing aldoxime ether- (**8a**–**c**) and ester-linked (**9a**–**f**) five-membered heterocycles.



8a–c



9a–f

Compd	R	IC_{50}[a] (μM)				
		H460	SW620	HepG2	MCF-7	HEK293T
8a		62±3	>100	5 ± 3	5 ± 3	7 ± 2
8b		>100	>100	6 ± 4	12 ± 2	33 ± 23
8c		>100	>100	41 ± 36	>100	>100
9a		>100	>100	>100	51 ± 23	>100
9b		>100	84 ± 12	44 ± 7	>100	25 ± 14
9c		59 ± 19	>100	4 ± 2	6 ± 3	13±0.4
9d		>100	>100	>100	>100	>100
9e		>100	>100	15 ± 9	12 ± 2	30 ± 19
9f		>100	>100	5 ± 2	>100	>100

[a] IC_{50}; the concentration that causes 50 % growth inhibition.

Electrochemical Properties of Selected Compounds by Voltammetry Assays

The electrochemical properties of **8a**, **8b**, **9c** and **9f**, with potent and selective antiproliferative activity, were investigated by cyclic voltammetry in acetonitrile solution (0.1 M Et_4NClO_4), using GC as a working electrode. Figures 5 and 6 show cyclic voltammograms for the oxidation of ester- and aldoxime ether-linked disubstituted ferrocene derivatives recorded at a scan rate of 100 mV s^{-1}, within the potential range from 0.0 to 1.4 V. Cyclic voltammetry measurements showed that all compounds provided a similar voltammetry response, i.e., it consists of one pair of redox peaks (A1/C1) at about 0.3 V, followed by two anodic peaks, A2 at about 0.85 V and A3 at around 1.10 V (Table 3).

The peak-to-peak separation between A1 and C1 exceeds 60/n mV (where *n* is the number of transferred electrons), indicating a (quasi)reversible one-electron oxidation

Table 3. Values of oxidation (A1, A2, and A3) and reduction (C1) CV potentials for compounds **8a**, **8b**, **9c**, and **9f** in CH_3CN (0.1 mol/L Et_4NClO_4) on a GC electrode. The scan rate is 100 mV s^{-1}.

Cmpd	**8a**	**8b**	**9c**	**9f**
E_pA1 / V	0.30	0.31	0.30	0.30
E_pC1 / V	0.21	0.23	0.23	0.23
E_pA2 / V	0.84	0.83	0.85	0.86
E_pA3 / V	1.15	1.07	1.10	1.10

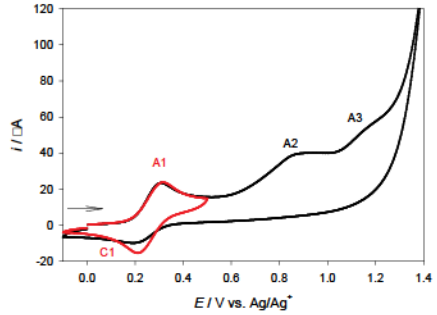


Figure 5. Cyclic voltammogram of a 1 mmol L^{-1} solution of compound **8a** recorded in CH_3CN containing 0.1 M Et_4NClO_4 at a glassy carbon (GC) electrode. The scan rate was 100 mV s^{-1}. The solid red line represents the cyclic voltammogram of compound **8a** in the potential range from 0 to 0.5 V, while the dotted line corresponds to the supporting electrolyte. The arrow indicates the direction of the potential sweep.

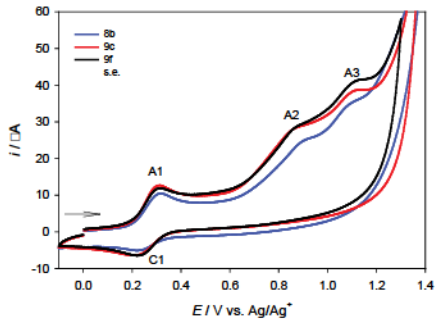


Figure 6. Cyclic voltammograms of 0.5 mmol L^{-1} solutions of compounds **8b**, **9c**, and **9f** recorded in CH_3CN containing 0.1 M Et_4NClO_4 at a glassy carbon (GC) electrode. The scan rate was 100 mV s^{-1}. The dotted curve represents the cyclic voltammogram of the supporting electrolyte, while the arrow indicates the direction of the potential sweep.

process of the ferrocene moiety, described by the redox couple $[Fe^{II}(C_5H_5)_2] \rightleftharpoons [Fe^{III}(C_5H_5)_2]^+ + e^-$.[44,45,55–57] Furthermore, closer inspection of the voltammograms of the investigated compounds, which contain additional triazole groups besides the Fc core, indicates that the oxidation peaks (A2 and A3) are most likely related to a complex oxidation process of the nitrogen atoms in the triazole ring located near the Fc core. Comparison of the voltammograms of all tested compounds (Figure 6) reveals that the nature of the substituents attached to the triazole ring does not influence these oxidation potentials.

However, deeper insight into the origin of these peaks as well as the mechanisms of their electrochemical oxidation, is beyond the scope of this study. Further research is required to fully understand the charge-transfer mechanism in these compounds.

CONCLUSION

In this study, a series of novel mono- and disubstituted ferrocene–heterocycle hybrids bearing ester- or aldoxime ether-linked five-membered heterocycles were synthesized using an efficient and environmentally benign Cu(I)-catalyzed 1,3-dipolar cycloaddition under mechanochemical liquid-assisted grinding conditions. This approach provided the targeted 1,2,3-triazolyl ferrocene derivatives in high yields for monosubstituted compounds, while the disubstituted analogs were obtained in somewhat lower yields. X-ray studies of **5b**, **6c**, **6d** and **6f** showed that the conformation of cyclopentadienyl (Cp) rings ranges from nearly eclipsed in **6d** to halfway between eclipsed and staggered in **5b**. Notable differences were also observed in the conformations of the Cp ring pendant moieties. Regarding their supramolecular assembling, C–H···N and C–H···O hydrogen bonds in **6c** and **6d**, supported by C–H···π and π···π interactions, form two-dimensional networks. In **6f**, the C–H···N hydrogen bonds, C–H···π and π···π interactions generate three-dimensional network, while the same supramolecular architecture in **5b** is built solely by C–H···π and π···π interactions. Biological evaluation showed that introducing a second triazolyl-linked heterocyclic substituent significantly enhanced antiproliferative activity, particularly against HepG2 and MCF-7 cancer cell lines. Among the investigated compounds, aldoxime ether-linked disubstituted derivatives exhibited the most pronounced cytotoxic effects, with compound **8a** showing strong but nonselective activity in the low micromolar range (HepG2: IC_{50} = 5 μM, SI = 1.4; MCF-7: IC_{50} = 5 μM, SI = 1.4). Notably, within the ester-linked disubstituted series, compound **9c** exhibited the highest antiproliferative potency, but was less selective (HepG2: IC_{50} = 4 μM, SI = 3.3; MCF-7: IC_{50} = 6 μM, SI = 2.2) than **9f**. In contrast, compound **9f** emerged as the most promising candidate, combining potent antiproliferative activity against HepG2 (IC_{50} = 5 μM) cells with high selectivity toward cancer cells over normal HEK293T cells (IC_{50} > 100 μM, SI > 20). Overall, these findings highlight the critical influence of the number of triazolyl units, substitution pattern, linker type, and the heterocyclic moiety on the modulation of biological activity. Electrochemical studies confirmed that all examined compounds retain the characteristic ferrocene redox behavior, undergoing a quasi-reversible one-electron oxidation of the ferrocene core followed by additional irreversible oxidation processes likely associated with the triazole unit. To further elucidate the mechanisms underlying the potent and selective antiproliferative activity of **9f** against HepG2 cells, further investigation of its ability to induce apoptosis and modulate intracellular ROS levels is warranted.

Acknowledgment. We greatly appreciate the financial support of the Croatian Science Foundation under the project HRZZ-IP-2022-10-9420.

Supplementary Information. Supporting information to the paper is attached to the electronic version of the article at: https://doi.org/10.5562/cca4278.

PDF files with attached documents are best viewed with Adobe Acrobat Reader which is free and can be downloaded from Adobe's web site.

REFERENCES

[1] P. Štěpnička, *Dalt. Trans.* **2022**, *51*, 8085–8102. https://doi.org/10.1039/D2DT00903J

[2] A. Straube, L. Useini, E. Hey-Hawkins, *Chem. Rev.* **2025**, *125*, 3007–3058. https://doi.org/10.1021/acs.chemrev.4c00295

[3] A. Singh, I. Lumb, V. Mehra, V. Kumar, *Dalt. Trans.* **2019**, *48*, 2840–2860. https://doi.org/10.1039/c8dt03440k

[4] V. Kovač, T. Lukačević, D. Jadreško, J. Mrvčić, D. Stanzer, K. Hanousek-Čiča, T. Murati, M. Miletić, I. Kmetič, *Appl. Organomet. Chem.* **2025**, *39*, e7753. https://doi.org/10.1002/aoc.7753

[5] Y. Wang, P. Pigeon, M. J. McGlinchey, S. Top, G. Jaouen, *J. Organomet. Chem.* **2017**, *829*, 108–115. https://doi.org/10.1016/j.jorganchem.2016.09.005

[6] Q. Zhang, X. Fan, H. Qian, S. Xiao, Q. Song, Y. Wang, J. Wang, S. Yang, Y. Wang, *Inorg. Chem. Front.* **2025**, *12*, 2368–2386. https://doi.org/10.1039/d4qi03268c

[7] W. Yang, J. Wen, X. Liu, J. Liu, *J. Inorg. Biochem.* **2025**, *269*, 112899. https://doi.org/10.1016/j.jinorgbio.2025.112899

[8] A. Kalamatianou, C. Ludwig, S. Zhong, K. Cariou, G. Gasser, *Chem. Soc. Rev.* **2025**, *54*, 3930–3961. https://doi.org/10.1039/d4cs01216j

[9] M. Patra, G. Gasser, *Nat. Rev. Chem.* **2017**, *1*, 0066. https://doi.org/10.1038/s41570-017-0066

[10] A. Chaudhary, K. Poonia, *Inorg. Chem. Commun.* **2021**, *134*, 109044. https://doi.org/10.1016/j.inoche.2021.109044

[11] S. Peter, B. A. Aderibigbe, *Molecules* **2019**, *24*, 3604. https://doi.org/10.3390/molecules24193604

[12] A. Sharma, R. Rana, N. Kumar, Jyoti, A. Khanna, H. K. Gulati, Pooja, S. Kaur, J. V. Singh, P. M. S. Bedi, *Inorg. Chem. Commun.* **2025**, *175*, 114155. https://doi.org/10.1016/j.inoche.2025.114155

[13] L. Guyon, A. Ladaycia, A. Bosio, L. Lemaire, F. Franconi, B. Lelièvre, N. Lautram, P. Pigeon, G. Jaouen, C. Passirani, E. Lepeltier, *Nanoscale* **2025**, *17*, 9232–9244. https://doi.org/10.1039/d5nr00643k

[14] G. Jaouen, A. Vessières, S. Top, *Chem. Soc. Rev.* **2015**, *44*, 8802–8817. https://doi.org/10.1039/c5cs00486a

[15] M. Cybulski, O. Michalak, W. Buchowicz, M. Mazur, *Molecules* **2024**, *29*, 4903. https://doi.org/10.3390/molecules29204903

[16] E. Navarrete, P. Morales, T. Caceres, A. Vega, P. Mesdom, K. Cariou, F. Godoy, G. Gasser, E. Flores, C. Mascayano, *Inorg. Chem.* **2025**, *64*, 3495–3505. https://doi.org/10.1021/acs.inorgchem.4c05103

[17] I. R. Latarissa, M. A. Khairinisa, G. N. Iftinan, A. Meiliana, I. P. Sormin, M. I. Barliana, K. Lestari, *Clin. Pharmacol. Adv. Appl.* **2025**, *17*, 1–11. https://doi.org/10.2147/CPAA.S493750

[18] J. Yan, K. Yue, X. Fan, X. Xu, J. Wang, M. Qin, Q. Zhang, X. Hou, X. Li, Y. Wang, *Eur. J. Med. Chem.* **2023**, *246*, 115004. https://doi.org/10.1016/j.ejmech.2022.115004

[19] R. Wang, H. Chen, W. Yan, M. Zheng, T. Zhang, Y. Zhang, *Eur. J. Med. Chem.* **2020**, *190*, 112109. https://doi.org/10.1016/j.ejmech.2020.112109

[20] A. Ranjan, D. Sharma, A. K. Srivastava, A. Varma, M. S. K. Jayadev, R. K. Joshi, *J. Organomet. Chem.* **2022**, *979*, 122500. https://doi.org/10.1016/j.jorganchem.2022.122500

[21] F. N. Sayed, G. G. Mohamed, *J. Organomet. Chem.* **2022**, *977*, 122450. https://doi.org/10.1016/j.jorganchem.2022.122450

[22] P. Bansode, D. Pore, S. Tayade, S. Patil, P. Choudhari, G. Rashinkar, *Results Chem.* **2023**, *5*, 100758. https://doi.org/10.1016/j.rechem.2022.100758

[23] M. Mazur, K. Ziemkiewicz, K. Rawiak, K. Kisiel, P. Wińska, K. Deresz, K. N. Jarzembska, W. Buchowicz, *Eur. J. Inorg. Chem.* **2022**, *10*, e202101098. https://doi.org/10.1002/ejic.202101098

[24] A. Batool, W. Rashid, K. Fatima, S. U. Khan in *Drug Resistance in Cancer: Mechanisms and Strategies*, (Eds.: S. U. Khan, F. Malik), Springer Nature Singapore, Singapore, **2024**, pp. 31–75. https://doi.org/10.1007/978-981-97-1666-1_2

[25] R. Peng, J.-J. Zhong, D. Yang, Z. Hong, H.-D. Bian, F.-P. Huang, *Appl. Organomet. Chem.* **2025**, *39*, e7960. https://doi.org/10.1002/aoc.7960

[26] W. Li, J. Yu, J. Wang, X. Fan, X. Xu, H. Wang, Y. Xiong, X. Li, X. Zhang, Q. Zhang, X. Qi, P. Pigeon, Q. Gu, J. Bruno-Colmenarez, G. Jaouen, M. J. McGlinchey, X. Qiu, S. L. You, J. Li, Y. Wang, *Chem. Sci.* **2024**, *15*, 10477–10490. https://doi.org/10.1039/d4sc02002b

[27] J. Zheng, L. Zeng, M. Tang, H. Lin, C. Pi, R. Xu, X. Cui, *Int. J. Mol. Sci.* **2021**, *22*, 1–13. https://doi.org/10.3390/ijms22063097

[28] V. Bhardwaj, D. Gumber, V. Abbot, S. Dhiman, P. Sharma, *RSC Adv.* **2015**, *5*, 15233–15266. https://doi.org/10.1039/c4ra15710a
[29] E. Mateev, M. Georgieva, A. Zlatkov, *J. Pharm. Pharm. Sci.* **2022**, *25*, 24–40. https://doi.org/10.18433/JPPS32417
[30] G. P. Oliveira, M. A. Lima, G. B. S. Pereira, A. R. Costa, A. A. Batista, M. R. Forim, M. R. Cominetti, R. D. Zanetti, R. L. Farias, A. V. G. Netto, J. H. Araujo-Neto, J. A. Ellena, L. Olmedo-Moreno, V. Capilla-Gonzalez, F. V. Rocha, *J. Mol. Struct.* **2025**, *1322*, 1–12. https://doi.org/10.1016/j.molstruc.2024.140306
[31] F. M. Sroor, H. K. A. Elhakim, S. M. Abdelrehim, K. F. Mahrous, A. F. El-Sayed, I. A. Abdelhamid, *J. Mol. Struct.* **2025**, *1321*, 140001. https://doi.org/10.1016/j.molstruc.2024.140001
[32] S. Thakur, D. Kumar, S. Jaiswal, K. K. Goel, P. Rawat, V. Srivastava, S. Dhiman, H. R. Jadhav, A. R. Dwivedi, *RSC Med. Chem.* **2024**, *16*, 481–510. https://doi.org/10.1039/d4md00450g
[33] Q. Guan, Z. Gao, Y. Chen, C. Guo, Y. Chen, H. Sun, *Eur. J. Med. Chem.* **2024**, *275*, 116578. https://doi.org/10.1016/j.ejmech.2024.116578
[34] K. Bozorov, J. Zhao, H. A. Aisa, *Bioorg. Med. Chem.* **2019**, *27*, 3511–3531. https://doi.org/10.1016/j.bmc.2019.07.005
[35] T. Kosmalski, A. Hetmann, R. Studzińska, S. Baumgart, D. Kupczyk, K. Roszek, *Molecules* **2022**, *27*, 1374. https://doi.org/10.3390/molecules27041374
[36] J. Fotie, C. M. Matherne, J. B. Mather, J. E. Wroblewski, K. Johnson, L. G. Boudreaux, A. A. Perez, *Int. J. Mol. Sci.*, **2023**, *24*, 16854. https://doi.org/10.3390/ijms242316854
[37] H. L. Qin, J. Leng, C. P. Zhang, I. Jantan, M. W. Amjad, M. Sher, M. Naeem-Ul-Hassan, M. A. Hussain, S. N. A. Bukhari, *J. Med. Chem.* **2016**, *59*, 3549–3561. https://doi.org/10.1021/acs.jmedchem.6b00276
[38] C. P. Jackson, S. Fang, S. R. Benjamin, T. Alayi, Y. Hathout, S. M. Gillen, J. P. Handel, B. M. Brems, J. M. Howe, L. N. Tumey, *Bioorg. Med. Chem. Lett.* **2022**, *75*, 128953. https://doi.org/10.1016/j.bmcl.2022.128953
[39] R. Sheyi, B. G. de la Torre, F. Albericio, *Pharmaceutics* **2022**, *14*, 396. https://doi.org/10.3390/pharmaceutics14020396
[40] S. Maračić, S. Jakopec, M. Piškor, M. Leventić, J. Lapić, S. Djaković, M. Cetina, L. Glavaš-Obrovac, S. Raić-Malić, *Appl. Organomet. Chem.* **2023**, *37*, e7124. https://doi.org/10.1002/aoc.7124
[41] S. Djaković, L. Glavaš-Obrovac, J. Lapić, S. Maračić, J. Kirchofer, M. Knežević, M. Jukić, S. Raić-Malić, *Appl. Organomet. Chem.* **2021**, *35*, 1–16. https://doi.org/10.1002/aoc.6052
[42] S. Maračić, J. Lapić, S. Djaković, T. Opačak-Bernardi, L. Glavaš-Obrovac, V. Vrček, S. Raić-Malić, *Appl. Organomet. Chem.* **2019**, *33*, e4628. https://doi.org/10.1002/aoc.4628
[43] S. Jakopec, L. Gourdon-Grünewaldt, I. Čipor, A. Meščić Macan, B. Perić, I. Piantanida, K. Cariou, G. Gasser, S. I. Kirin, S. Raić-Malić, *Dalt. Trans.* **2023**, *52*, 9482–9498. https://doi.org/10.1039/d3dt01070h
[44] V. Rep, M. Piškor, H. Šimek, P. Mišetić, P. Grbčić, J. Padovan, V. Gabelica Marković, D. Jadreško, K. Pavelić, S. Kraljević Pavelić, S. Raić-Malić, *Molecules* **2020**, *25*, 1570. https://doi.org/10.3390/molecules25071570
[45] S. Jakopec, N. Pantalon Juraj, A. Brozovic, D. Jadreško, B. Perić, S. I. Kirin, S. Raić-Malić, *Appl. Organomet. Chem.* **2022**, *36*, 1–22. https://doi.org/10.1002/aoc.6575
[46] S. Chandrappa, M. Umashankara, K. Vinaya, C. S. Ananda Kumar, K. S. Rangappa, *Tetrahedron Lett.* **2012**, *53*, 2632–2635. https://doi.org/10.1016/j.tetlet.2012.03.052
[47] M. Jumppanen, S. M. Kinnunen, M. J. Välimäki, V. Talman, S. Auno, T. Bruun, G. Boije Af Gennäs, H. Xhaard, I. B. Aumüller, H. Ruskoaho, J. Yli-Kauhaluoma, *J. Med. Chem.* **2019**, *62*, 8284–8310. https://doi.org/10.1021/acs.jmedchem.9b01086
[48] J. M. Casas-Solvas, E. Ortiz-Salmerón, J. J. Giménez-Martínez, L. García-Fuentes, L. F. Capitán-Vallvey, F. Santoyo-González, A. Vargas-Berenguel, *Chem. – A Eur. J.* **2009**, *15*, 710–725. https://doi.org/10.1002/chem.200800927
[49] G. Singh, S. Rani, *Appl. Organomet. Chem.* **2018**, *32*, 1–13. https://doi.org/10.1002/aoc.4028
[50] M. Szigeti, Z. Dobi, T. Soós, *J. Org. Chem.* **2018**, *83*, 2869–2874. https://doi.org/10.1021/acs.joc.8b00014
[51] T. Mosmann, *J. Immunol. Methods* **1983**, *65*, 55–63. https://doi.org/10.1016/0022-1759(83)90303-4
[52] I. Cortés, A. M. Sarotti, *Org. Biomol. Chem.* **2023**, *21*, 2935–2940. https://doi.org/10.1039/d3ob00291h
[53] E. Abele, E. Lukevics, *Khim. Geterotsikl. Soedin.* **2001**, *37*, 141–169. https://doi.org/10.1023/A:1017559314561
[54] P. Ying, J. Yu, W. Su, *Adv. Synth. Catal.* **2021**, *363*, 1246–1271. https://doi.org/10.1002/adsc.202001245
[55] N. S. Neghmouche, A. Khelef, T. Lanez, *J. Fundam. Appl. Sci.* **2009**, *1*, 23–30. https://doi.org/10.4314/jfas.v1i2.3
[56] S. M. Batterjee, M. I. Marzouk, M. E. Aazab, M. A. El-Hashash, *Appl. Organomet. Chem.* **2003**, *17*, 291–297. https://doi.org/10.1002/aoc.414
[57] A. M. Bond, E. A. McLennan, R. S. Stojanovic, F. G. Thomas, *Anal. Chem.* **1987**, *59*, 2853–2860. https://doi.org/10.1021/ac00151a007